

**REPORT FOR OPEN LAB PROJECT**  
**MEASURING SLIPSTREAM DRAG**

Prepared by: Team D1T21  
Gabriel Kurfman [gkurfman@purdue.edu](mailto:gkurfman@purdue.edu)  
Miguel Ojeda [ojeda4@purdue.edu](mailto:ojeda4@purdue.edu)  
Jacob Saxton [saxtonj@purdue.edu](mailto:saxtonj@purdue.edu)

School of Mechanical Engineering,  
Purdue University  
585 Purdue Mall  
West Lafayette, IN 47907

Date: 2025.04.29

Submitted to: Prof. Jun Chen

## 1 INTRODUCTION

This project aims to identify the aerodynamic benefits of “slipstreaming” a passenger vehicle behind a semi-truck trailer. Slipstreaming, also known as “drafting”, is a technique where an automobile follows closely behind another to reduce aerodynamic drag by taking advantage of the low-pressure wake created by the lead vehicle. This technique is commonly used in motorsports [1], but it is also feasible (albeit dangerous) for a passenger vehicle to slipstream behind large trucks on the highway. This investigation is personally compelling as it combines fundamental fluid dynamics principles with practical applications for improving vehicle fuel economy. We aim to measure the coefficient of drag on the trailing vehicle at various separation distances and speeds to determine the conditions for drag reduction.

In theory, a vehicle slipstreaming can be considered to have a lower drag coefficient  $C_d$  due to the reduction in air speed in the wake behind the semi-truck and the transition of the fluid from laminar to turbulent. This affects the magnitude of the drag force on the car  $F_d$ , as seen in **Eq. 1**,

$$F_d = \frac{1}{2} \rho V^2 A C_d \quad (1)$$

where  $\rho$  is the fluid density,  $V$  is the velocity, and  $A$  is the cross-sectional area. By experimentally measuring values of  $F_d$ , we can derive a relationship between separation distance and  $C_d$  to validate the hypothesis.

The team used a test model to simulate this real-life scenario. Some of the assumptions used in the experiment were incompressible and uniform flow, surface friction is negligible, the models were rigid, atmospheric conditions are constant, and the boundary layer effects from the wind tunnel were negligible.

## 2 OBJECTIVE

This lab is designed to accomplish the following objectives: (1) Define the relationship between the drag force and the separation distance of a car and a semi-truck. (2) Determine the impact wind speed has on slipstreaming. (3) Deduce the most efficient distance and speed to slipstream behind a semi-truck.

## 3 METHOD

### 3.1 *Experiment Facility*

The facility used to conduct this experiment is the low-speed open-circuit wind tunnel (ELD, model 402B) located in the ME30801 lab. The dimensions of its test section are 61 cm (length)  $\times$  30.5 cm (width)  $\times$  30.5 cm (height). The wind speeds are controlled from a range of 3 m/s to 48 m/s with the help of a centrifugal belt-driven fan with 12.40-inch wheel diameter. Wind speed can be adjusted with a Variable Frequency Driver (VFD). The test models were placed in the wind tunnel on an adjustable ground plate to simulate flat highway conditions [2]. A photo of the wind tunnel facility is provided in **Fig. 1**.

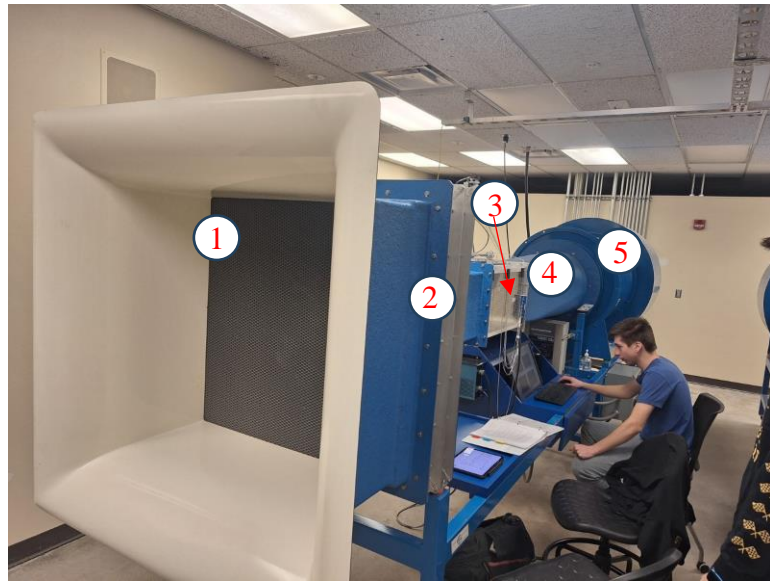


**Fig 1.** low-speed open-circuit wind tunnel (ELD, model 402B). 1) Intake and Honeycomb. 2) Contraction. 3) Test Section. 4) Diffuser. 5) Fan and Exit.

The coordinate system used for this experiment exclusively utilizes an x-axis to measure the distance between the car and the rear end of the semi-truck. The origin of the coordinate system starts at the tip of the model car. The flow direction is on the negative x-axis direction, as seen below in **Fig. 2**.

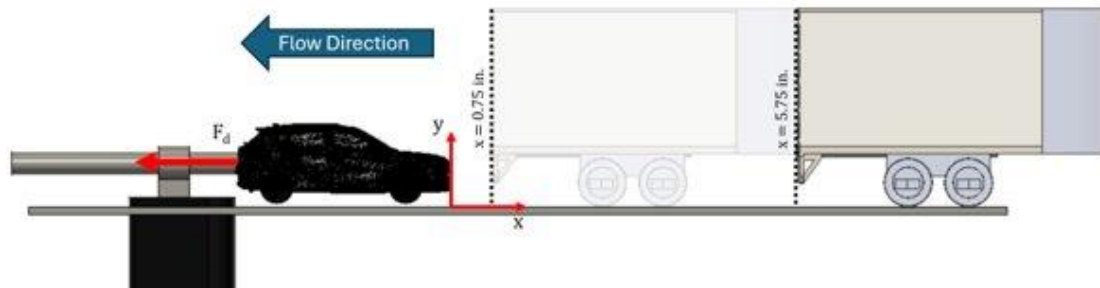


**Fig 2.** Coordinate system

### 3.2 Test Model

This experiment uses two different scale models for the semi-truck trailer and passenger vehicle. Both have been scaled 1:50 (1 ft. = 0.24 in.) to fit within the wind tunnel test section.

The trailer used is a 48' Dry Van available on the GrabCAD library [3], printed using standard PLA. The original file was modified to shorten the truck body, add a curved nose, and include imbedded nut slots in the wheels. To mount the trailer, four #10 screws are threaded under the ground plate into the imbedded nuts. At the instructor's discretion, the team machined additional holes into the plate to mount the trailer at 1 in. increments.

The passenger vehicle used is a Moskvich 3 Sehol X4 [4] and is also 3D printed. To mount the passenger vehicle in the wind tunnel, a 3/8-16 threaded rod is installed through a hole in rear face, screwing onto an imbedded nut slotted into the body. The overall layout is illustrated in **Fig 3**.

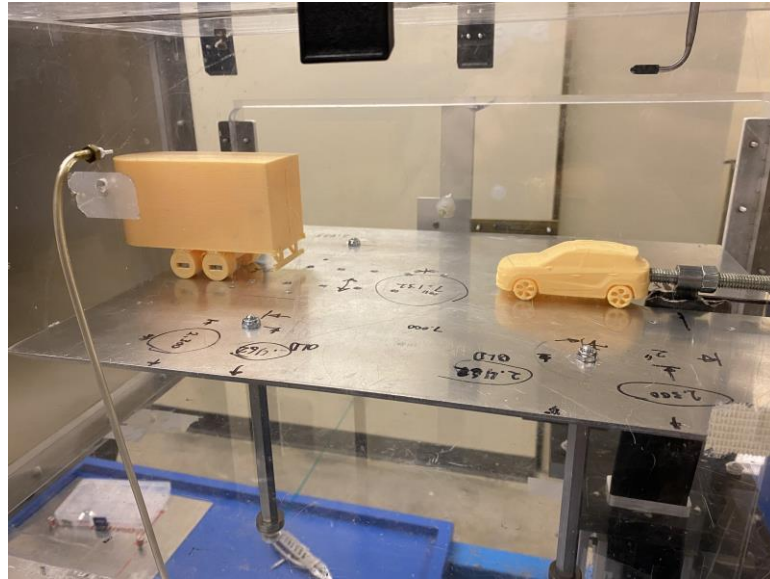


**Fig 3.** Models mounted in wind tunnel with ground plate

More technical details on the models and ground plate can be found in the CAD drawings in **Appendix B**.

### 3.3 *Instrumentation*

For this experiment, a dynamometer was used to measure the drag force applied to the car. The selected model is a linear voltage differential transform (LVDT). The LVDT used can measure both drag and lift by using mechanical deflections on the beams and then corresponding this into electrical values. The sensor can read measurements from 0 N to 100 N. The signals acquired from the sensor can be converted into force by using **Eq. 2**:

$$F_d = K [ (V_{total} - V_{0,offset\ total}) - (V_{ts} - V_{0,ts\_offset,ts}) ] \quad (2)$$

where  $F$  is the modified force in N,  $K$  is the calibration constant,  $V_{total}$  is the reading total voltage at test condition.  $V_{0,offset\ total}$  is the voltage reading at zero wind tunnel test condition in V.  $V_{ts}$  is the voltage reading with test stand only at test condition between 30-60 Hz in V.  $V_{0,ts\_offset,ts}$  is the voltage reading at zero wind speed with stand-only at 0 Hz in V.

A National Instrument Data Acquisition System (National Instrument USB-6341) is used to read the pressure data from the pressure scanner and position data from the probe traversing system.

Additionally, a mercury barometer and thermometer are used to measure the air density and viscosity at the time of the experiment. The mercury barometer balances between atmospheric pressure and a vacuum, giving pressure reading in mmHg. The thermometer works on the principle of thermal expansion and provides a temperature reading in degrees Celsius. A correction factor is then applied to obtain the absolute atmospheric pressure. This is then converted to density using the ideal gas law rearranged for density, **Eq. 3**.

$$\rho = \frac{P}{RT} \quad (3)$$

### 3.4 Experimental Conditions

The experimental data was collected on 4/16/25. Utilizing the measurement equipment and equations detailed above, the following pressure and room temperature were recorded as shown in **Table 1**. The predetermined lift and drag scaling factors were also recorded and can be seen in **Appendix C**.

**Table 1** Room Conditions

Temperature (C)	Height of Hg (mm)	Corrected Pressure (kPa)
22.0	752.0	99.90

In this experiment, it was determined after careful consideration that matching the Reynolds number to real-world conditions was not practically feasible. Due to the proportional scaling of velocity and characteristic dimension in **Eq. 4**, matching the characteristics between the 3D printed models and full-scale vehicles would require a substantially larger test section area or maximum wind speed.

$$R_e = \frac{\rho V_0 D}{\mu} \quad (4)$$

To compromise, the experiment used wind speeds in the same range as highway speeds, normal situations in which a vehicle encounters a semi-truck. The difference between the experimental Reynold's number and the full-scale number can be seen in **Table 2** below.

**Table 2.** Experimental Reynold's Numbers

MPH	$R_e$ (Experiment)	$R_e$ (Theoretical full-scale)
40	101,200	5,018,700
60	151,800	7,528,000
80	202,300	10,037,400

For use in the wind tunnel VFD, the desired wind speeds must be converted to an electrical signal in Hertz. Using the linear relation specified in the wind tunnel manual [5], the frequency values used in this experiment are listed in **Table 3**.

**Table 3.** Wind Speed to real speed relation

MPH	m/s	Hz
40	17.9	24.6
60	26.8	35.2
80	35.8	45.8

One final parameter unique to this experiment is the variation of the following distance between the vehicle and truck. The ideal distances were determined from approximate highway tailgating lengths, scaled 1:50 to match the scale of the model vehicles. The distance increments can be seen in **Table 4** below.

**Table 4.** Following distance increments

Experimental “D” (in.)	Full-Scale “D” (ft.)
0.75	3.125
1.75	7.292
2.75	11.458
3.75	15.625
4.75	19.792
5.75	23.958
$\infty$	$\infty$ (control, no trailer)

In this experiment, several assumptions were made to simplify the data processing:

- The flow around the semi-truck is steady and uniform in the wind tunnel test section
- Air behaves as an incompressible fluid within the testing range of wind speeds
- Surface friction effects on the ground plate are neglected.
- The models are rigidly mounted without vibration affecting measurements
- Atmospheric conditions (temperature and pressure) remain constant during each set of measurements
- Boundary layer effects from the wind tunnel walls do not significantly affect the flow around the vehicles

### 3.5 Procedures

To set up the test, the ground plate is inserted into the wind tunnel test section. The passenger vehicle is then installed via the threaded rod and adjusted so that its wheels are close to the ground plate but not touching it. Then, the trailer is installed into the plate at the first separation distance.

To begin data collection, the wind tunnel can be set to the first desired speed so that drag readings can be measured. The readings are then saved, and the wind tunnel speed is adjusted to each of the other desired points. After all data for the set location is recorded, the fan is stopped to change the location of the truck and the car. This process is repeated for all locations and checked off the data sheet shown in **Appendix C**. In this case the speeds selected were 40, 60 and 80 MPH. The locations were made from 0.75 in. with increments of 1.00 in. to 5.75 in. was reached on the model. An additional set of measurements were obtained where the car and truck are removed for calibration, as well as at 0 MPH for a baseline voltage measurement.

## 4 RESULTS

After gathering the data for drag forces at each truck distance and wind speed, the results were plotted for visualization. Each plot is shown with respect to the truck-vehicle separation, normalized to one vehicle length. The data is also presented as a change from the baseline value (no truck at all, acting as “infinite separation”).

First, we can examine the slipstream effect on the drag force at each individual speed (**Fig. 4-6**). The error bars in these plots are one standard deviation of the raw voltage data sampled from the LVDT, scaled by the calibration factor.

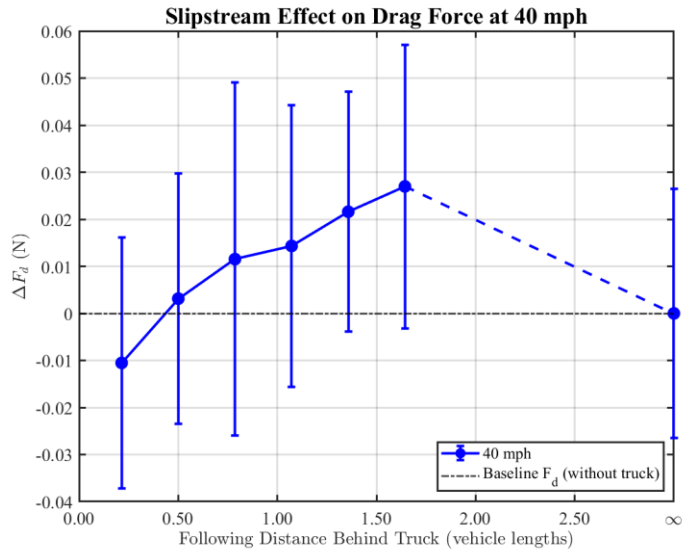


**Fig 4.** Force change vs. following distance at 40 MPH. Error bars indicate one standard deviation.

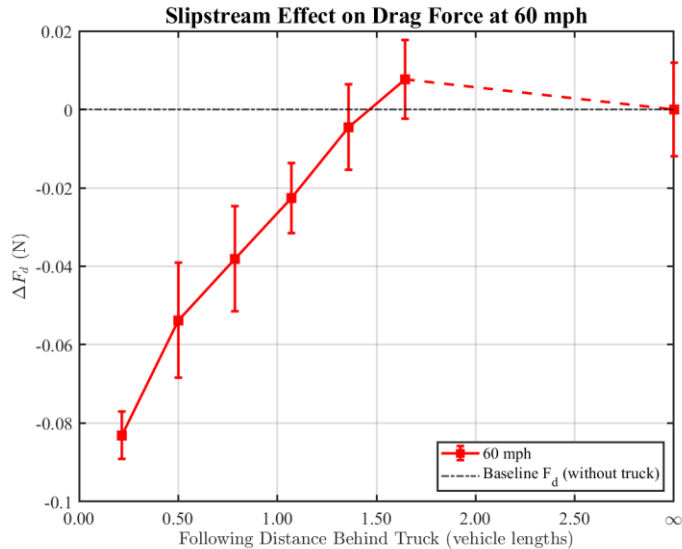


**Fig 5.** Force change vs. following distance at 60 MPH. Error bars indicate one standard deviation.

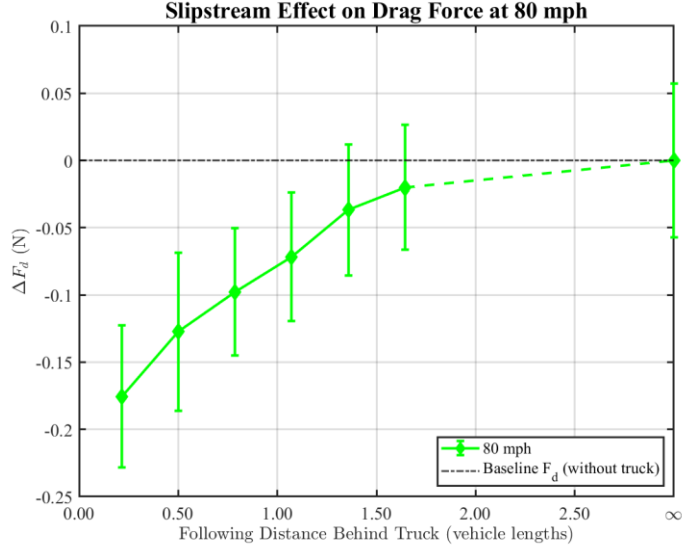


**Fig 6.** Force change vs. following distance at 80 MPH. Error bars indicate one standard deviation.

Each of these individual plots shows a clear trend of larger forces as the following distance increases. This can also be illustrated on a combined plot of the force at all three different speeds, as shown in **Fig 7**. One interesting slipstream effect that can be seen in this graph is that at lower speeds, the change in force is less prevalent. In fact, at 40 MPH the drag force was larger with the truck present than the baseline for most separation distances.

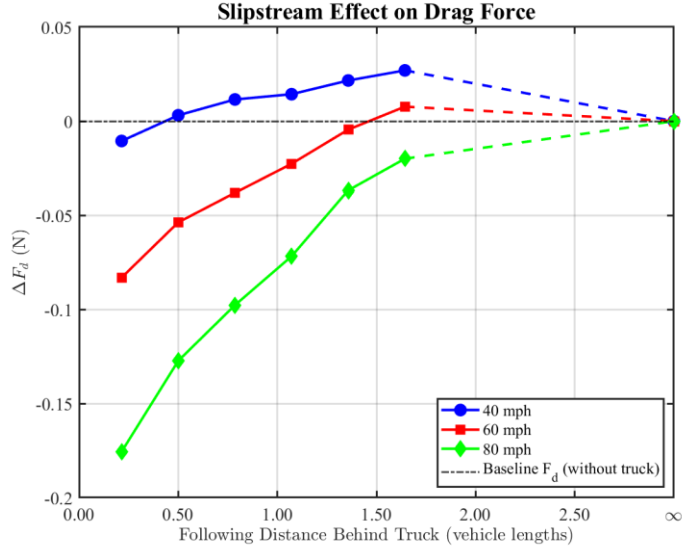


**Fig 7.** Combined force change vs. following distance.

We can also plot the coefficient of drag of the model to better understand how these trends might apply to a full-scale vehicle. The typical drag coefficient equation was rearranged to solve for  $C_d$  using **Eq. 5** with the cross-sectional area derived from the CAD model of  $8.71 \times 10^{-4} \text{ m}^2$ . The density and velocity were both based on the experimental conditions outlined in **Section 3.4**.

$$C_d = \frac{2F_d}{\rho V^2 A} \quad (5)$$

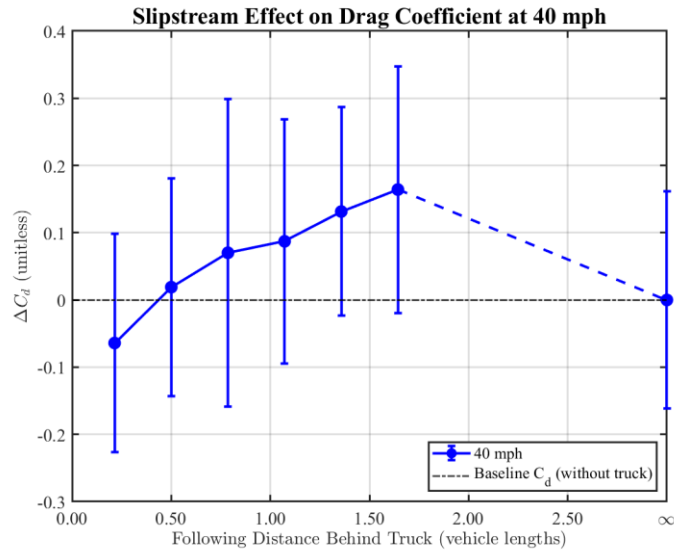


**Fig 8.** Drag coefficient change vs. following distance at 40 MPH. Error bars indicate one standard deviation.

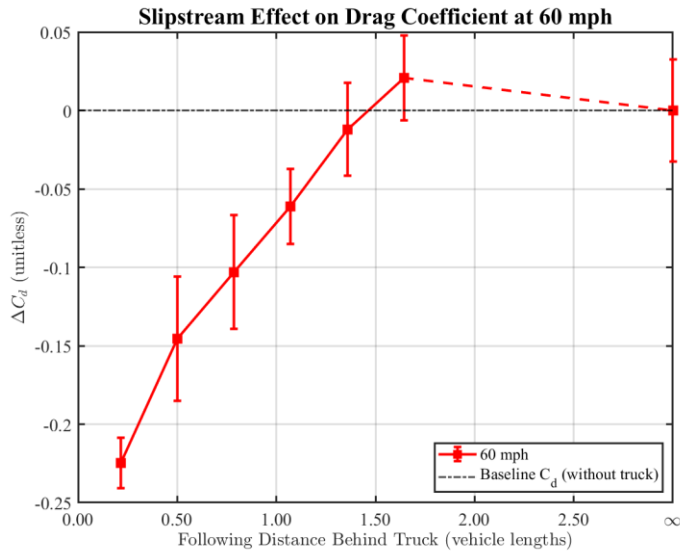


**Fig 9.** Drag coefficient change vs. following distance at 60 MPH. Error bars indicate one standard deviation.

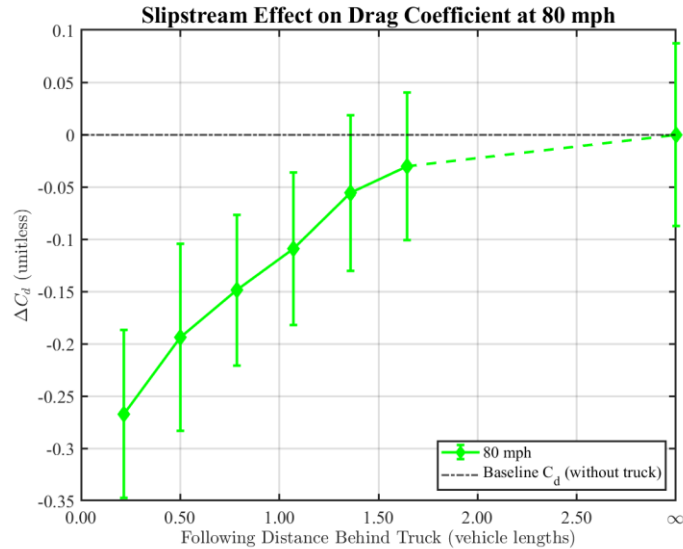


**Fig 10.** Drag coefficient change vs. following distance at 80 MPH. Error bars indicate one standard deviation.

Just as with the drag force plots, it is easier to visualize these trends on a combined graph, shown in **Fig. 11**. It is apparent that when the vehicle is following closely behind the truck, the coefficient of drag is reduced (as much as -0.27) in our experiment. The effect is less prevalent at slower speeds, with the 40 MPH experiment increasing the  $C_d$  for most distances. This is proportional to the changes observed in the drag force plots above.

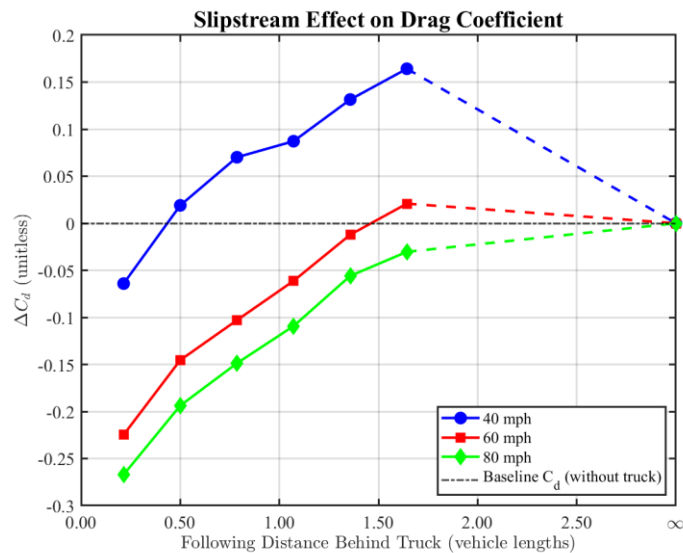


**Fig 11.** Combined force change vs. following distance.

## 5 DISCUSSION

As expected, the closer a car is positioned behind a semi-truck, the less drag force it experiences. This is due to the vehicle traveling within the semi-truck's wake flow, where the air pressure is lower, and the turbulent flow reduces the aerodynamic resistance acting on the following car. Therefore, the most optimal position to minimize the drag force is directly behind the semi-truck, within its slipstream. The semi-truck's wake significantly alters the airflow around the following vehicle, decreasing the pressure difference across the car and reducing overall drag.

As the speed of the system increases, the drag force on the drafting car decreases when it is positioned inside the truck's slipstream. This happens because the slipstream becomes larger at higher speeds, creating a lower-pressure zone behind the truck. A stronger, larger slipstream at higher speeds means that even if the drafting car is slightly farther back, it can still experience a significant reduction in air resistance. This reduces the air resistance on the car, leading to a lower drag force and a lower drag coefficient compared to no trailer. So, higher speeds amplify the drafting effect, making it more forgiving in terms of following distance while still achieving drag reduction.

This experiment had several limitations that must be considered. First, the experimental equipment was not ideal. The small size of the wind tunnel restricted the scale of both the truck and car models, making it impossible to match the Reynolds number to real-world conditions. Second, the LVDT sensor had a precision of  $\pm 0.5$  N, which reduced the accuracy of the force measurements. As seen in **Fig 12**, the drag measurements recorded are far less than 0.5 N and the error makes it difficult to quantify exact values. It did, however, still allow for the identification of clear trends, as shown in the results section with plot of the change in force and coefficient of drag with respect to the baseline. Finally, the truck model was simplified to ensure it could fit within the wind tunnel, which did not allow for a fully accurate representation of real aerodynamic behavior.

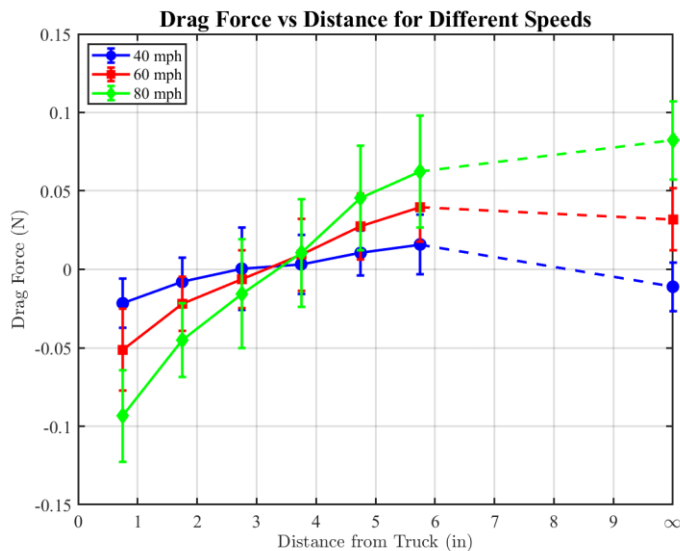


**Fig 12.** Raw data from experiment showing force values well below LVDT precision

Therefore, it can be mentioned that the three objectives for this report were achieved. The relationship between drag force and the semi-truck distance was defined: the closer the car gets to the truck the lower the drag force on the car became. It was also determined that the slipstreaming effect was more prevalent at higher wind speeds. Finally, it was found that the smaller the car-truck separation distance was, the more effective the slipstreaming was.

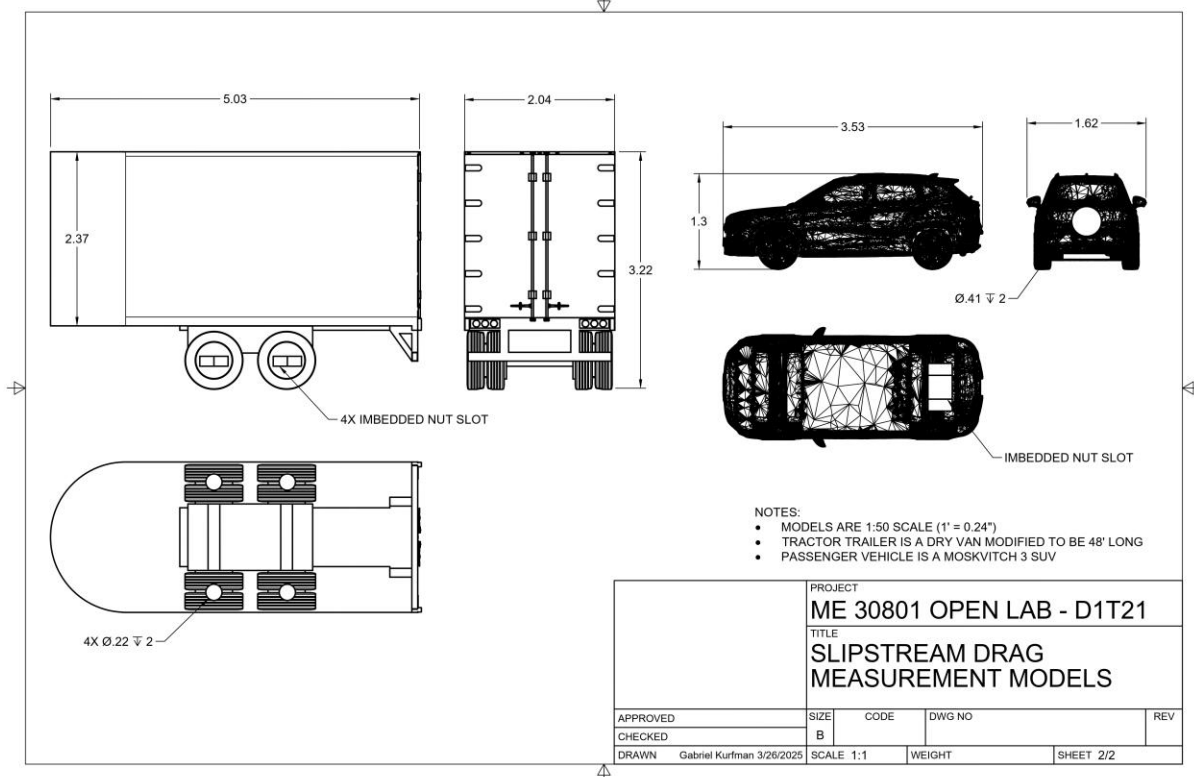
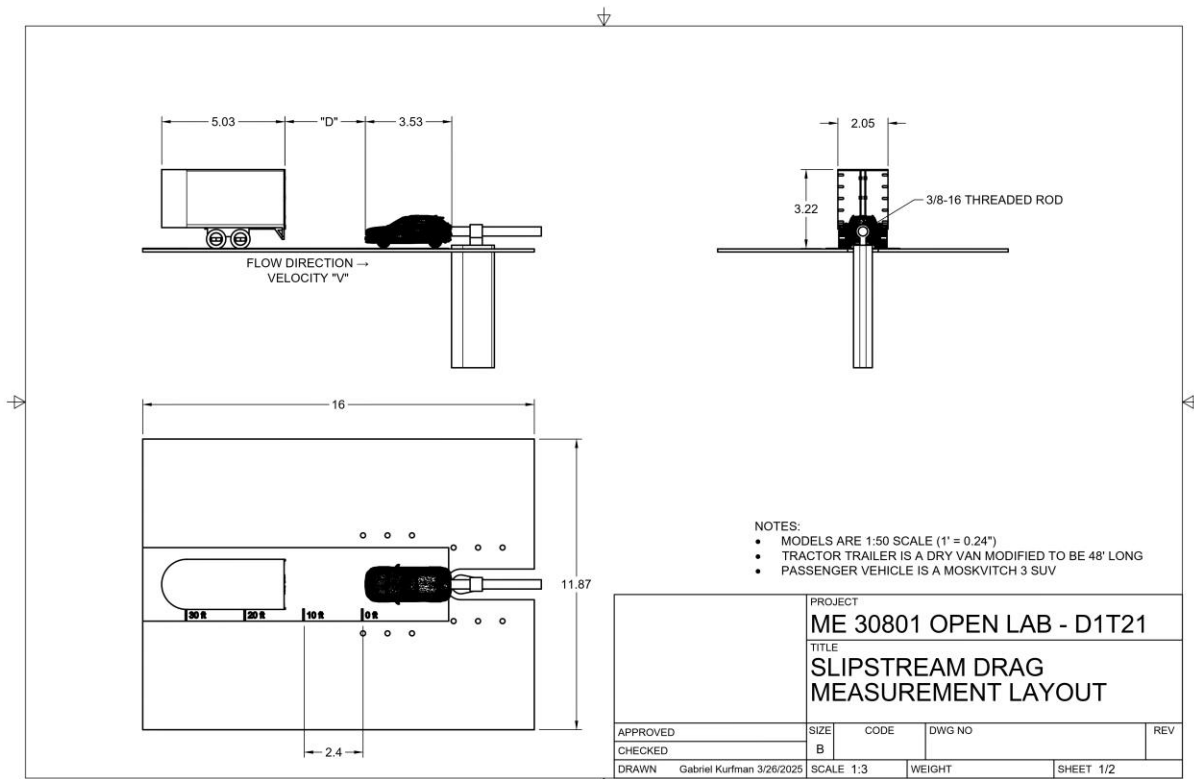
## REFERENCES

- [1] Halliday, N. (2023, November 28). Aerodynamic drafting (slipstreaming) in racing. SimScale. <https://www.simscale.com/blog/drafting-slipstreaming-in-racing/>
- [2] Jun Chen (2025, February 25). Open lab: logistic support. Brightspace. <https://purdue.brightspace.com/d2l/home/1222985>
- [3] Don Phillips (2024, October 1). Dry van trailer 53 feet [3D model]. GrabCAD. <https://grabcad.com/library/dry-van-trailer-53-feet-1>
- [4] Aleksey Tsyrik (2024, October 5). Moskvich 3 (JAC JS4) Sehol X4 [3D model]. GrabCAD. <https://grabcad.com/library/moskvich-3-jac-js4-sehol-x4-1>
- [5] Purdue University, S. of M. E. (2025). *ME30801: FLUID MECHANICS LAB MODEL TESTS IN WIND TUNNEL*.

**APPENDIX****APPENDIX A: CONTRIBUTION OF TEAM MEMBERS**

Item\Name	Kurzman, Gabriel	Ojeda, Miguel	Saxton, Jacob	Subtotal
<b>Project Idea</b>	34%	33%	33%	100%
<b>Proposal Preparation</b>	50%	30%	20%	100%
<b>Lab Test</b>	34%	33%	33%	100%
<b>Data Processing</b>	100%			100%
<b>Report Writing</b>				
Introduction	80%	20%		100%
Objective			100%	100%
Method		50%	50%	100%
Results	100%			100%
Discussion	10%	40%	50%	100%
Edit & Proofread	34%	33%	33%	100%
<b>PPT preparation</b>	70%	15%	15%	100%

## APPENDIX B: CAD DRAWINGS



## APPENDIX C: DATA SHEET

Separation Distance (in)	Speed = 0 Hz	Speed = 24.6 Hz	Speed = 35.2 Hz	Speed = 45.8 Hz	Scaling Factor	Value
0.75		✓	✓	✓	Drag	11.196
1.75		✓	✓	✓	Lift	80.856
2.75		✓	✓	✓		
3.75		✓	✓	✓		
4.75		✓	✓	✓		
5.75		✓	✓	✓		
6.75		✓	✓	✓		
$\infty$ (control, no trailer)	✓	✓	✓	✓		
Calibration (no vehicle)	✓	✓	✓	✓		